Article

A Time Two-mesh Finite Difference Numerical Scheme for the Symmetric Regularized Long Wave Equation

Jingying Gao*, Siriguleng He*, Qingmei Bai and Jie Liu

School of Mathematics and Big Data, Hohhot Minzu College, Hohhot 010051, China; minzugjy@sina.com
* Correspondence: minzugjy@sina.com(J.G.); cmml2005@163.com(S.H.)

Abstract: This paper proposed a time two-mesh (TT-M) finite difference numerical scheme to improve the efficiency of solving the symmetric regularized long wave (SRLW) equation. The TT-M Crank-Nicolson discretization and finite difference method are employed in time and space approximation respectively. The scheme involves three main steps: firstly, the time interval is divided into coarse and fine time meshes, then the nonlinear system is solved on the coarse time mesh; secondly, coarse numerical solutions on the fine time mesh are computed using an interpolation formula based on the solutions derived in the step one; lastly, the TT-M finite difference numerical solutions can be obtained through constructing the linearized fine time mesh system using Taylor's formula. Compared to the currently existing TT-M numerical methods, the novelty of this study is that the nonlinear term including derivatives is linearized by Taylor's formula for a function with three variables, whose error analysis is more complex. Finally, some numerical examples, including computational time and accuracy, preservation of conservation laws, are given to verify the efficiency of the scheme. By comparing it with the standard nonlinear finite difference scheme, this method can reduce CPU time without sacrificing accuracy.

Keywords: SRLW equation; finite difference; time two-mesh; convergence analysis; conservation law

1. Introduction

The regularized long wave (RLW) equation [1,2] is a nonlinear partial differential equation that mainly describes the evolution of waves in shallow water channels and ion acoustic etc. It is a simplified version of the more complex Korteweg-de Vries (KdV) equation [3], which includes higher-order nonlinearities and dispersion effects. The symmetric regularized long wave (SRLW) equation [4] is a modified version of the RLW equation that includes a symmetry-breaking term. This term allows for the formation of asymmetric solutions, making the SRLW equation a more realistic model for waves in shallow water channels.

In this paper, the following initial boundary value problem of the SRLW equation is considered:

$$\begin{cases} u_t + \rho_x + uu_x - u_{xxt} = 0, \quad x_L \le x \le x_R, \ 0 < t \le T, \\ \rho_t + u_x = 0, \quad x_L \le x \le x_R, \ 0 < t \le T, \\ u(x_L,t) = u(x_R,t) = 0, \quad \rho(x_L,t) = \rho(x_R,t) = 0, \quad 0 < t \le T, \\ u(x,0) = u_0(x), \quad \rho(x,0) = \rho_0(x), \quad x_L \le x \le x_R. \end{cases} \tag{1}$$

The SRLW equation has attracted significant attention and has been extensively studied in the literatures. Numerous methods have been developed for obtaining numerical solutions to the SRLW equation, ranging from conservative finite difference schemes to mixed finite element methods. Wang et al. [5] proposed three conservative finite difference schemes that are all of second-order accuracy in both space and time. They also proved that the energy is preserved for all schemes while the mass is preserved only for the first scheme. Yimnet et al. [6] presented a novel finite difference method for the SRLW

 doi:10.20944/preprints202305.1973.v1

equation that utilizes a four-level average difference technique for solving the fluid velocity independently from the density. Hu et al. [7] developed a coupled conservative three-level implicit scheme that achieves a fourth–order rate of convergence. Li [8] considered a weighted and compact conservative difference scheme that is decoupled and linearized in practical computation, thus requiring only the solution of two tridiagonal systems of linear algebraic equations at each time step. Bai et al. [9] investigated a two-layer conservative finite difference scheme for the SRLW equation with homogeneous boundary conditions and analyzed the scheme's convergence and stability using a discrete functional analysis method. Xu et al. [10] applied a mixed finite element method to solve the dissipative SRLW equations with damping term. He et al. [11] developed a fourth-order accurate compact difference scheme for the SRLW equation for a single nonlinear velocity form and conducted theoretical analysis using the discrete energy method.

From the view of numerical calculation, the time two-mesh (TT-M) method combined with finite element method or finite difference method can also solve plenty of nonlinear partial differential equation with better computational efficiency. For instance, Liu et al. [12] proposed the fast TT-M finite element method to solve the fractional water wave model, which has also been applied to other fractional models. Yin et al. [13] developed the TT-M finite element algorithm to solve a space fractional Allen–Cahn model and discussed in detail the problem of parameter selection. The TT-M finite element method was utilized by Liu et al. [14] to numerically solve the two-dimensional Gray–Scott model with space fractional derivatives. Wen et al. [15] used the TT-M algorithm in combination with the H_1-Galerkin mixed finite element method to numerically solve the nonlinear distributed order diffusion model. The computational efficiency of the algorithm was demonstrated, and the theoretical results were verified by numerical examples with both smooth and non-smooth solutions. Tian et al. [16] developed the finite element method combined with the TT-M technique to solve the coupled Schrödinger–Boussinesq equations. In recent years, there has been a amount of research on using the combined TT-M and finite difference methods to solve partial differential equations. Qiu and Xu et al. [17,18] developed and analyzed a TT-M algorithm based on finite difference (FD) methods for solving nonlinear fractional partial differential equations. Similarly, Niu et al. [19] used the TT-M technique to propose a fast high-order compact difference scheme for the nonlinear distributed order fractional Sobolev model appearing in porous media. He et al. [20] further extended the application of the TT-M method by studying a time two-mesh high-order compact difference scheme for solving the nonlinear Schrödinger equation and the scheme of second-order convergence rate in time as well as fourth-order in space. Despite the extensive research on the TT-M method in various fields, to the best of our knowledge, no study on the application of the TT-M method combined with finite difference to the SRLW equation has been discovered. Hence, investigations on the TT-M finite difference method's performance when applied to the SRLW equation are still required.

The main contributions of this paper are as follows: (i) A novel TT-M finite difference numerical approach, incorporating a TT-M Crank-Nicolson algorithm for time discretization and finite difference method for space approximation, has been proposed to solve the SRLW equation. (ii) The TT-M finite difference method is used for the first time to solve partial differential equation with nonlinear term including derivatives. (iii) The detailed proofs of convergence analysis of the scheme are given, which are more complicated than existing methods. (iv) Numerical examples have been provided to demonstrate the computational speed and accuracy of the proposed method, which outperforms standard nonlinear finite difference method.

The remaining part of this article is organized as follows. In Section 2, some notations and useful lemmas are given. In Section 3, the TT-M finite difference numerical scheme is presented. In Section 4, the convergence of the scheme is analyzed. In Section 5, some numerical results are provided to test the theoretical results, computational efficiency of the scheme. Finally, in Section 6, we provide a brief conclusion.

Preprints (www.preprints.org) | NOT PEER-REVIEWED | Posted: 29 May 2023 doi:10.20944/preprints202305.1973.v1

2. Notations and Some Lemmas

As usual, the time interval $(0,T]$ and spatial interval $[x_L,x_R]$ are divided into N and J uniform partitions. The following notations will be used in this paper:

$$\left(u_j^n\right)_x=\frac{u_{j+1}^n-u_j^n}{h},\quad \left(u_j^n\right)_{\bar{x}}=\frac{u_j^n-u_{j-1}^n}{h},\quad \left(u_j^n\right)_{\hat{x}}=\frac{u_{j+1}^n-u_{j-1}^n}{2h},$$
$$\left(u_j^n\right)_t=\frac{u_j^{n+1}-u_j^n}{\tau},\quad u_j^{n+\frac{1}{2}}=\frac{1}{2}(u_j^{n+1}+u_j^n),\quad \left(u_j^n\right)_{x\bar{x}}=\frac{u_{j+1}^n-2u_j^n+u_{j-1}^n}{h^2},$$

where τ,h denote the uniform time and spatial step length respectively, $x_j=x_L+jh, j=0,1,2,\cdots,J, t_n=n\tau, n=1,2,\cdots,[T/\tau]=N$, superscript n denotes a quantity associated with the time level t_n, subscript j denotes a quantity associated with space mesh point x_j. In this paper, M denotes general constant, which may have different value in different place.

Since $u\to 0$ for $x\to+\infty$ or $x\to-\infty$, we may assume $u_{-1}=u_{J+1}=0, 1\le n\le N$ for simplicity, where $j=-1$ and $J+1$ are ghost points. Let $H_{h,0}$ denote the set of mesh functions u^n defined on I_h with boundary conditions $u_{-1}^n=u_0^n=u_J^n=u_{J+1}^n=0$. For any two mesh functions $u^n,w^n\in H_{h,0}$, we define the discrete inner product and norms as follows:

$$(u^n,w^n)=h\sum_{j=1}^{J-1}u_j^nw_j^n,\quad \|u^n\|=\sqrt{(u^n,u^n)},\quad \|u^n\|_\infty=\max_{1\le j\le J-1}\left|u_j^n\right|.$$

Next, we presented some useful lemmas.

Lemma 1. *(See [11]). For any mesh functions $u^n,w^n\in H_{h,0}$, we have*

$$(a)(u_x^n,w^n)=-(u^n,w_{\bar{x}}^n)=-(u^n,w_x^n),\quad (b)(u_{x\bar{x}}^n,w^n)=-(u_x^n,w_x^n),\quad (c)(u_{\hat{x}}^n,w^n)=-(u^n,w_{\hat{x}}^n).$$

Lemma 2. *(See [20,21]). Assume that a sequence of nonnegative real numbers $\{a_j\}_{j=0}^{\infty}$ satisfying*

$$a_{n+1}\le\alpha+\beta\sum_{j=0}^{n}a_j\tau,\quad n\ge 0,$$

then there has the inequality $a_{n+1}\le(\alpha+\tau\beta a_0)e^{\beta(n+1)\tau}$, where $\alpha\ge 0,\beta$ and τ are positive constants.

Lemma 3. *(See [9,21]). For any discrete mesh function $u^n\in H_{h,0}$, there exists constants C_1 and C_2, such that*

$$\|u^n\|_\infty\le C_1\|u^n\|+C_2\|u_x^n\|.$$

3. The TT-M Finite Difference Scheme

In this paper, we studied a TT-M finite difference fast numerical method for the SRLW equation (1). In order to give the TT-M finite difference scheme, firstly, the time interval $(0,T]$ is partitioned uniformly into P coarse time intervals and then each coarse time interval is divided into $s(2\le s\in Z^+)$ fine time intervals. The coarse time mesh with the nodes $t_{ks}=k\tau_C(k=1,\ldots,P)$ satisfying $0=t_0<t_s<t_{2s}<\cdots<t_{Ps}=T$ and the fine time mesh with the nodes $t_n=n\tau_F(n=1,2,\ldots,Ps=N)$ satisfying $0=t_0<t_1<t_2<\cdots<t_{Ps}=T$, where $\tau_C=s\tau_F$ and τ_F are the coarse time and the fine time step size, respectively.

Secondly, the truncation errors of the problem (1) is considered, let $v_j^n=u(x_j,t_n)$, $\varphi_j^n=\rho(x_j,t_n)$ be the exact solutions of $u(x,t)$ and $\rho(x,t)$ in term of the point (x_j,t_n), then we have

Preprints (www.preprints.org) | NOT PEER-REVIEWED | Posted: 29 May 2023 doi:10.20944/preprints202305.1973.v1

$$Er_j^n = (v_j^n)_t + (\varphi_j^{n+1})_{\hat{x}} - (v_j^n)_{x\bar{x}t} + \frac{1}{3}\left\{ v_j^{n+\frac{1}{2}}(v_j^{n+\frac{1}{2}})_{\hat{x}} + \left[(v_j^{n+\frac{1}{2}})^2\right]_{\hat{x}} \right\}, \tag{2}$$

$$Es_j^n = (\varphi_j^n)_t + (v_j^n)_{\hat{x}}, \tag{3}$$

$$\begin{aligned} &v_0^n = v_J^n = 0, \varphi_0^n = \varphi_J^n = 0, \\ &v_j^0 = v_0(x_L + jh), \varphi_j^0 = \varphi_0(x_L + jh). \end{aligned}$$

By Taylor series expansion, we have

$$\begin{aligned} Er_j^n &= (u_t + \rho_x - u_{xxt} + uu_x)_{(x_j,t_n)} = O(h^2 + \tau), \\ Es_j^n &= (\rho_t + u_x)_{(x_j,t_n)} = O(h^2 + \tau). \end{aligned}$$

Next, based on equations (2) and (3), a TT-M finite difference scheme for problem (1) is constructed with three steps.

Step 1: On the coarse time mesh, let $u_{C,j}^{ks} = u(x_j, t_{ks}), \rho_{C,j}^{ks} = \rho(x_j, t_{ks})$ be the numerical solutions of of $u(x,t)$ and $\rho(x,t)$ in term of the point (x_j, t_{ks}), then coarse time nonlinear finite difference scheme is given as

$$(u_{C,j}^{ks})_t + (\rho_{C,j}^{(k+1)s})_{\hat{x}} - (u_{C,j}^{ks})_{x\bar{x}t} + \frac{1}{3}\left\{ u_{C,j}^{ks+\frac{1}{2}}(u_{C,j}^{ks+\frac{1}{2}})_{\hat{x}} + \left[(u_{C,j}^{ks+\frac{1}{2}})^2\right]_{\hat{x}} \right\} = 0, \tag{4}$$

$$(\rho_{C,j}^{ks})_t + (u_{C,j}^{ks})_{\hat{x}} = 0, \tag{5}$$

$$\begin{aligned} &u_{C,0}^{ks} = u_{C,J}^{ks} = 0, \rho_{C,0}^{ks} = \rho_{C,J}^{ks} = 0, && k = 0, 1, \ldots, P, \\ &u_{C,j}^{0} = u_0(x_L + jh), \rho_{C,j}^{0} = \rho_0(x_L + jh), && j = 1, 2, \ldots, J-1, \end{aligned}$$

where $u_{C,j}^{ks+\frac{1}{2}} = \frac{1}{2}(u_{C,j}^{(k+1)s} + u_{C,j}^{ks})$.

Step 2: Based on the solutions u_C^{ks}, ρ_C^{ks} at time levels t_{ks} obtained from step 1, we apply the Lagrange's linear interpolation formula to compute $u_C^{ks-l}, \rho_C^{ks-l}$ at time levels $t_{ks-l} (l = 1, 2, \ldots, s-1$ and $k = 1, 2, \ldots, P, ks - l = n)$, we have

$$u_C^{ks-l} = \frac{t_{ks-l} - t_{ks}}{t_{(k-1)s} - t_{ks}} u_C^{(k-1)s} + \frac{t_{ks-l} - t_{(k-1)s}}{t_{ks} - t_{(k-1)s}} u_C^{ks} = \frac{l}{s} u_C^{(k-1)s} + (1 - \frac{l}{s}) u_C^{ks}, \tag{6}$$

$$\rho_C^{ks-l} = \frac{t_{ks-1} - t_{ks}}{t_{(k-1)s} - t_{ks}} \rho_C^{(k-1)s} + \frac{t_{ks-1} - t_{(k-1)s}}{t_{ks} - t_{(k-1)s}} \rho_C^{ks} = \frac{l}{s} \rho_C^{(k-1)s} + (1 - \frac{l}{s}) \rho_C^{ks}. \tag{7}$$

Remark 1. *The equation (7) is only employed for theoretical analysis of the scheme. In numerical simulation, the coarse numerical solutions ρ_C^{ks-l} are no need to compute since it does not used in step 3.*

Step 3: Based on all the coarse numerical solutions $u_{C,j}^n (n = 0, 1, 2, \ldots, Ps = N, j = 1, 2, \ldots, J-1)$ obtained in the first two steps, Taylor's formula is used to construct a linearized system on the fine time mesh, which is expressed as follows. Let $u_{F,j}^n = u(x_j, t_n), \rho_{F,j}^n = \rho(x_j, t_n)$ be the numerical solutions of $u(x,t)$ and $\rho(x,t)$ in term of the point (x_j, t_n) on the fine time mesh, then

Preprints (www.preprints.org) | NOT PEER-REVIEWED | Posted: 29 May 2023 doi:10.20944/preprints202305.1973.v1

$$
\begin{aligned}
&(u_{F,j}^{n})_t + (\rho_{F,j}^{n+1})_{\hat{x}} - (u_{F,j}^{n})_{x\bar{x}t} + \frac{1}{6h}\Big[f(u_{C,j-1}^{n+\frac{1}{2}}, u_{C,j}^{n+\frac{1}{2}}, u_{C,j+1}^{n+\frac{1}{2}}) \\
&+ f_x(u_{C,j-1}^{n+\frac{1}{2}}, u_{C,j}^{n+\frac{1}{2}}, u_{C,j+1}^{n+\frac{1}{2}})(u_{F,j-1}^{n+\frac{1}{2}} - u_{C,j-1}^{n+\frac{1}{2}}) \\
&+ f_y(u_{C,j+1}^{n+\frac{1}{2}}, u_{C,j}^{n+\frac{1}{2}}, u_{C,j+1}^{n+\frac{1}{2}})(u_{F,j}^{n+\frac{1}{2}} - u_{C,j}^{n+\frac{1}{2}}) \\
&+ f_z(u_{C,j-1}^{n+\frac{1}{2}}, u_{C,j}^{n+\frac{1}{2}}, u_{C,j+1}^{n+\frac{1}{2}})(u_{F,j+1}^{n+\frac{1}{2}} - u_{C,j+1}^{n+\frac{1}{2}})\Big] = 0,
\end{aligned} \tag{8}
$$

$$
(\rho_{F,j}^{n})_t + (u_{F,j}^{n})_{\hat{x}} = 0, \tag{9}
$$

$$
\begin{aligned}
&u_{F,0}^{n} = u_{F,J}^{n} = 0, \quad \rho_{F,0}^{n} = \rho_{F,J}^{n} = 0, \\
&u_{F,j}^{0} = u_0(x_L + jh), \quad \rho_{F,j}^{0} = \rho_0(x_L + jh), \\
&j = 1, \ldots, J-1, \quad n = 0, 1, 2, \ldots, N,
\end{aligned}
$$

where $f(x,y,z) = (z-x)y + z^2 - x^2$ and

$$
f_x(x,y,z) = -y - 2x, f_y(x,y,z) = z - x, f_z(x,y,z) = y + 2z
$$

are the three partial derivatives of $f(x,y,z)$ with respect to x, y, z.

Remark 2. *Similar to the Gauss-Seidel method applied to linear systems, we have modified our method to improve the accuracy of fine mesh solutions u_F^{n+1} by using u_F^n in calculation.*

4. Convergence Analysis of the TT-M Finite Difference Scheme

The focus of this section is on performing convergence analysis of the nonlinear system specifically on the coarse time mesh.

Theorem 1. *Suppose that the exact solutions v^n, φ^n to the initial boundary value problem equation (1) is sufficiently smooth and let u_C^n, ρ_C^n be the numerical solutions on the coarse time mesh. Then,*

$$
\|v^n - u_C^n\|_\infty \le O(h^2 + \tau_C), \|\varphi^n - \rho_C^n\| \le O(h^2 + \tau_C).
$$

Proof. Denote $e_{C,j}^{ks} = v_j^{ks} - u_{C,j}^{ks}, \eta_{C,j}^{ks} = \varphi_j^{ks} - \rho_{C,j}^{ks}, 1 \le j \le J-1, 0 \le k \le P$. Subtracting equation (4) from equation (2) and equation (5) from equation (3), we obtain

$$
\begin{aligned}
Er_{C,j}^{ks} =& (e_{C,j}^{ks})_t + (\eta_{C,j}^{(k+1)s})_{\hat{x}} - (e_{C,j}^{ks})_{x\bar{x}t} \\
&+ \frac{1}{3}\left\{v_j^{ks+\frac{1}{2}}(v_j^{ks+\frac{1}{2}})_{\hat{x}} + \left[(v_j^{ks+\frac{1}{2}})^2\right]_{\hat{x}}\right\} - \frac{1}{3}\left\{u_{C,j}^{ks+\frac{1}{2}}(u_{C,j}^{ks+\frac{1}{2}})_{\hat{x}} + \left[(u_{C,j}^{ks+\frac{1}{2}})^2\right]_{\hat{x}}\right\},
\end{aligned} \tag{10}
$$

$$
Es_{C,j}^{ks} = (\eta_{C,j}^{ks})_t + (e_{C,j}^{ks})_{\hat{x}}. \tag{11}
$$

The proof contains two cases. Firstly, we consider the case of $n = ks (k = 0, 1, 2, \ldots, P)$, then $n+1 = (k+1)s$. The initial and boundary condition satisfies

$$
\begin{aligned}
&e_{C,j}^{0} = 0, \quad \eta_{C,j}^{0} = 0, \\
&u_{C,0}^{n} = u_{C,J}^{n} = 0, \quad \rho_{C,0}^{n} = \rho_{C,J}^{n} = 0.
\end{aligned}
$$

Preprints (www.preprints.org) | NOT PEER-REVIEWED | Posted: 29 May 2023 doi:10.20944/preprints202305.1973.v1

Taking the inner product $(\cdot,\cdot)$ on both sides of equation (10) with $e_C^{n+1}+e_C^n$, we have

$$\begin{aligned}(Er_C^n, e_C^{n+1}+e_C^n) &= ((e_C^{n+1})_t, e_C^n+e_C^n) + ((\eta_C^{n+1})_{\hat{x}}, e_C^{n+1}+e_C^n)\\ &-((e_C^n)_{x\bar{x}t}, e_C^{ks+1}+e_C^n) + h\sum_{j=1}^{J-1}(\mathrm{I}+\mathrm{II})(e_{C,j}^{n+1}+e_{C,j}^n),\end{aligned} \tag{12}$$

where

$$\mathrm{I}=\frac{1}{3}\left[v_j^{n+\frac{1}{2}}(v_j^{n+\frac{1}{2}})_{\hat{x}} - u_{C,j}^{n+\frac{1}{2}}(u_{C,j}^{n+\frac{1}{2}})_{\hat{x}}\right], \mathrm{II}=\frac{1}{3}\left\{\left[(v_j^{n+\frac{1}{2}})^2\right]_{\hat{x}} - \left[(u_{C,j}^{n+\frac{1}{2}})^2\right]_{\hat{x}}\right\}.$$

Notice that

$$((e_C^n)_t, e_C^{n+1}+e_C^n) = \frac{1}{\tau_C}(\|e_C^{n+1}\|^2 - \|e_C^n\|^2), \tag{13}$$

$$((\eta_C^{n+1})_{\hat{x}}, e_C^{n+1}+e_C^n) = -h\sum_{j=1}^{J-1}\left[\eta_{C,j}^{n+1}(e_{C,j}^{n+1}+e_{C,j}^n)_{\hat{x}}\right], \tag{14}$$

$$-((e_C^n)_{x\bar{x}t}, e_C^{n+1}+e_C^n) = \frac{1}{\tau_C}(\|e_{C,x}^{n+1}\|^2 - \|e_{C,x}^n\|^2), \tag{15}$$

$$\begin{aligned}h\sum_{j=1}^{J-1}\mathrm{I}\cdot(e_{C,j}^{n+1}+e_{C,j}^n) =& -\frac{2}{3}h\sum_{j=1}^{J-1}(e_{C,j}^{n+\frac{1}{2}}\cdot v_j^{n+\frac{1}{2}})_{\hat{x}}e_{C,j}^{n+\frac{1}{2}}\\ &-\frac{2}{3}h\sum_{j=1}^{J-1}(e_{C,j}^{n+\frac{1}{2}})_{\hat{x}}(e_{C,j+1}^{n+\frac{1}{2}}+e_{C,j-1}^{n+\frac{1}{2}})u_{C,j}^{n+\frac{1}{2}},\end{aligned} \tag{16}$$

$$\begin{aligned}h\sum_{j=1}^{J-1}\mathrm{II}\cdot(e_{C,j}^{n+1}+e_{C,j}^n) =& \frac{2}{3}h\sum_{j=1}^{J-1}(v_j^{n+\frac{1}{2}}\cdot e_{C,j}^{n+\frac{1}{2}})_{\hat{x}}e_{C,j}^{n+\frac{1}{2}}\\ &-\frac{2}{3}h\sum_{j=1}^{J-1}u_{C,j}^{n+\frac{1}{2}}e_{C,j}^{n+\frac{1}{2}}(e_{C,j}^{n+\frac{1}{2}})_{\hat{x}},\end{aligned} \tag{17}$$

then substituting equations (13)-(17) into (12), we have

$$\begin{aligned}\|e_C^{n+1}\|^2+\|e_{C,x}^{n+1}\|^2 &= \|e_C^n\|^2+\|e_{C,x}^n\|^2+\tau_C h\sum_{j=1}^{J-1}\left[\eta_{C,j}^{n+1}(e_{C,j}^{n+1}+e_{C,j}^n)_{\hat{x}}\right]\\ &+\frac{2}{3}\tau_C h\sum_{j=1}^{J-1}\left[(e_{C,j}^{n+\frac{1}{2}})_{\hat{x}}(e_{C,j+1}^{n+\frac{1}{2}}+e_{C,j-1}^{n+\frac{1}{2}})u_{C,j}^{n+\frac{1}{2}}+u_{C,j}^{n+\frac{1}{2}}e_{C,j}^{n+\frac{1}{2}}(e_{C,j}^{n+\frac{1}{2}})_{\hat{x}}\right]\\ &+\tau_C(Er_C^n, e_C^{n+1}+e_C^n).\end{aligned} \tag{18}$$

From Cauchy–Schwarz inequality, we obtain

$$(Er_C^n, e_C^{n+1}+e_C^n) \le \|Er_C^n\|^2 + \frac{1}{2}(\|e_C^{n+1}\|^2+\|e_C^n\|^2).$$

Using Lemma 1, the equation (18) can be rewritten as

$$\begin{aligned}\|e_C^{n+1}\|^2+\|e_{C,x}^{n+1}\|^2 &\le \|e_C^n\|^2+\|e_{C,x}^n\|^2\\ &+M\tau_C(\|\eta_C^{n+1}\|^2+\|e_C^{n+1}\|^2+\|e_C^n\|^2+\|e_{C,x}^{n+1}\|^2+\|e_{C,x}^n\|^2)+\tau_C\|Er_C^n\|^2.\end{aligned} \tag{19}$$

Preprints (www.preprints.org) | NOT PEER-REVIEWED | Posted: 29 May 2023 doi:10.20944/preprints202305.1973.v1

Similarly, taking the inner product $(\cdot,\cdot)$ on both sides of equation (11) with $\eta_C^{n+1}+\eta_C^n$, we obtain

$$\|\eta_C^{n+1}\|^2 = \|\eta_C^n\|^2 - \tau_C h\sum_{j=1}^{J-1}(e_{C,j}^n)_{\hat{x}}(\eta_{C,j}^{n+1}+\eta_{C,j}^n) + \tau_C(Es_C^n, \eta_C^{n+1}+\eta_C^n). \tag{20}$$

From Cauchy–Schwarz inequality, we have

$$(Es_C^n, \eta_C^{n+1}+\eta_C^n) \le \|Es_C^n\|^2 + \frac{1}{2}(\|\eta_C^{n+1}\|^2 + \|\eta_C^n\|^2).$$

Using Lemma 1, the equation (20) can be rewritten as

$$\|\eta_C^{n+1}\|^2 \le \|\eta_C^n\|^2 + M\tau_C(\|e_{C,x}^n\|^2 + \|\eta_C^{n+1}\|^2 + \|\eta_C^n\|^2) + \tau_C\|Es_C^n\|^2. \tag{21}$$

Add equations (19) and (21), we get

$$\begin{aligned}\|e_C^{n+1}\|^2 + \|e_{C,x}^{n+1}\|^2 + \|\eta_C^{n+1}\|^2 &\le \|e_C^n\|^2 + \|e_{C,x}^n\|^2 + \|\eta_C^n\|^2 \\ &+ M\tau_C(\|\eta_C^{n+1}\|^2 + \|\eta_C^n\|^2 + \|e_C^{n+1}\|^2 + \|e_C^n\|^2 + \|e_{C,x}^{n+1}\|^2 + \|e_{C,x}^n\|^2) \\ &+ \tau_C\|Er_C^n\|^2 + \tau_C\|Es_C^n\|^2.\end{aligned} \tag{22}$$

Let $B_C^n = \|e_C^n\|^2 + \|e_{C,x}^n\|^2 + \|\eta_C^n\|^2$, then equation (22) becomes

$$B_C^{n+1} - B_C^n \le M\tau_C(B_C^{n+1} + B_C^n) + M\tau_C(h^2+\tau_C)^2,$$

and obtain

$$(1-M\tau_C)(B_C^{n+1} - B_C^n) \le 2M\tau_C B_C^n + M\tau_C(h^2+\tau_C)^2.$$

By taking τ_C small enough so that $(1-M\tau_C) > \lambda > 0$, then

$$B_C^{n+1} - B_C^n \le M\tau_C B_C^n + M\tau_C(h^2+\tau_C)^2. \tag{23}$$

Summing from 0 to $P-1$ inequalities in equation (23), we have

$$B_C^P - B_C^0 \le M\tau_C\sum_{n=1}^{P-1} B_C^n + M\tau_C(h^2+\tau_C)^2,$$

and using Lemma 2, get

$$B_C^P \le [B_C^0 + M(h^2+\tau_C)^2]e^{MP\tau_C}. \tag{24}$$

From equation (24) and the initial and boundary condition, we have

$$\|e_C^n\| < O(h^2+\tau_C), \|e_{C,x}^n\| < O(h^2+\tau_C), \|\eta_C^n\| < O(h^2+\tau_C). \tag{25}$$

Then using Lemma 3, we obtain

$$\|e_C^n\|_\infty < O(h^2+\tau_C). \tag{26}$$

Secondly, we consider the case of $n = ks-l, (l = 1,2,\ldots,s-1$ and $k = 1,2,\ldots,P, ks-l = n)$. Based on the Lagrange's interpolation formula, we get

$$\begin{aligned}v^{ks-l} &= \frac{t_{ks-l}-t_{ks}}{t_{(k-1)s}-t_{ks}}v^{(k-1)s} + \frac{t_{ks-l}-t_{(k-1)s}}{t_{ks}-t_{(k-1)s}}v^{ks} \\ &= \frac{l}{s}v^{(k-1)s} + (1-\frac{l}{s})v^{ks} + \frac{v''(\theta_1)}{2}(t-t_{(k-1)s})(t-t_{ks}), \quad \theta_1 \in (t_{(k-1)s}, t_{ks}),\end{aligned} \tag{27}$$

Preprints (www.preprints.org) | NOT PEER-REVIEWED | Posted: 29 May 2023 doi:10.20944/preprints202305.1973.v1

$$\begin{aligned}\varphi^{ks-l} &= \frac{t_{ks-l}-t_{ks}}{t_{(k-1)s}-t_{ks}}\varphi^{(k-1)s}+\frac{t_{ks-l}-t_{(k-1)s}}{t_{ks}-t_{(k-1)s}}\varphi^{ks}\\ &= \frac{l}{s}\varphi^{(k-1)s}+(1-\frac{l}{s})\varphi^{ks}+\frac{\varphi''(\theta_2)}{2}(t-t_{(k-1)s})(t-t_{ks}),\quad \theta_2\in(t_{(k-1)s},t_{ks}).\end{aligned} \tag{28}$$

Subtracting equation (27) from (6), we have

$$\begin{aligned}v^{ks-l}-u_C^{ks-l} =&\frac{l}{s}(v^{(k-1)s}-u_C^{(k-1)s})+(1-\frac{l}{s})(v^{ks}-u_C^{ks})\\ &+\frac{v''(\theta_1)}{2}(t-t_{(k-1)s})(t-t_{ks}).\end{aligned}$$

Subtracting equation (28) from (7), we obtain

$$\begin{aligned}\varphi^{ks-l}-\rho_C^{ks-l} =&\frac{l}{s}(\varphi^{(k-1)s}-\rho_C^{(k-1)s})+(1-\frac{l}{s})(\varphi^{ks}-\rho_C^{ks})\\ &+\frac{\varphi''(\theta_2)}{2}(t-t_{(k-1)s})(t-t_{ks}).\end{aligned}$$

Using (25), (26) and triangle inequality, we conclude

$$\|e_C^{ks-l}\|_\infty \le O(h^2+\tau_C), \|\eta_C^{ks-l}\| \le O(h^2+\tau_C).$$

We obtain the result of Theorem 1 by synthesizing the aforementioned two cases. Next, we give the convergence analysis of the scheme on the fine time mesh. □

Theorem 2. *Suppose that the exact solutions v^n, φ^n to the initial boundary value problem equation (1) is sufficiently smooth and let u_F^n, ρ_F^n be the numerical solutions on the fine time mesh. Then,*

$$\|v^n-u_F^n\|_\infty \le O(h^2+\tau_C^2+\tau_F), \|\varphi^n-\rho_F^n\| \le O(h^2+\tau_C^2+\tau_F).$$

proof. Assume $e_{F,j}^n = v_j^n - u_{F,j}^n, \eta_{F,j}^n = \varphi_j^n - \rho_{F,j}^n, 1\le j\le J-1, 0\le n\le N$, Subtracting equation (8) from equation (2) and equation (9) from equation (3), we obtain

$$Er_{F,j}^n = (e_{F,j}^n)_t + (\eta_{F,j}^{n+1})_{\hat{x}} - (e_{F,j}^n)_{x\bar{x}t} + \frac{1}{6h}[(f_x e_{F,j-1}^{n+\frac{1}{2}} + f_y e_{F,j}^{n+\frac{1}{2}} + f_z e_{F,j+1}^{n+\frac{1}{2}}) + Q], \tag{29}$$

$$Es_{F,j}^n = (\eta_{F,j}^n)_t + (e_{F,j}^n)_{\hat{x}}, \tag{30}$$

where

$$\begin{aligned}Q =&\frac{1}{2}[(f_{xx}(e_{C,j-1}^{n+\frac{1}{2}})^2 + f_{yy}(e_{C,j}^{n+\frac{1}{2}})^2 + f_{zz}(e_{C,j+1}^{n+\frac{1}{2}})^2]\\ &+[f_{xy}e_{C,j-1}^{n+\frac{1}{2}}e_{C,j}^{n+\frac{1}{2}} + f_{xz}e_{C,j-1}^{n+\frac{1}{2}}e_{C,j+1}^{n+\frac{1}{2}} + f_{yz}e_{C,j}^{n+\frac{1}{2}}e_{C,j+1}^{n+\frac{1}{2}}],\end{aligned}$$

and $f_{xx}=f_{xx}(\xi,\varepsilon,\delta), f_{yy}=f_{yy}(\xi,\varepsilon,\delta), f_{zz}=f_{zz}(\xi,\varepsilon,\delta), f_{xy}=f_{xy}(\xi,\varepsilon,\delta), f_{xz}=f_{xz}(\xi,\varepsilon,\delta), f_{yz}=f_{yz}(\xi,\varepsilon,\delta)$ are the second order partial derivatives of $f(x,y,z), \xi\in(v_{j-1}^n, u_{C,j-1}^n), \varepsilon\in(v_j^n, u_{C,j}^n), \delta\in(v_{j+1}^n, u_{C,j+1}^n)$.

Taking the inner product $(\cdot,\cdot)$ on both sides of equation (29) with $e_F^{n+1}+e_F^n$, we have

$$\begin{aligned}\|e_F^{n+1}\|^2 + \|e_{F,x}^{n+1}\|^2 = \|e_F^n\|^2 + \|e_{F,x}^n\|^2 + \tau_F h\sum_{j=1}^{J-1}\left\{\eta_{F,j}^{n+1}\left[(e_{F,j}^{n+1})_{\hat{x}} + (e_{F,j}^n)_{\hat{x}}\right]\right\}\\ -\frac{\tau_F}{3}\sum_{j=1}^{J-1}(f_x e_{F,j-1}^{n+\frac{1}{2}} + f_y e_{F,j}^{n+\frac{1}{2}} + f_z e_{F,j+1}^{n+\frac{1}{2}})e_{F,j}^{n+\frac{1}{2}} - \frac{\tau_F}{3}\sum_{j=1}^{J-1}Qe_{F,j}^{n+\frac{1}{2}} + 2\tau_F(Er_F^n, e_F^{n+\frac{1}{2}}).\end{aligned} \tag{31}$$

Preprints (www.preprints.org) | NOT PEER-REVIEWED | Posted: 29 May 2023 doi:10.20944/preprints202305.1973.v1

Using $f_y = \frac{1}{2}(f_x + f_z)$ and $f_{xx} = -2, f_{yy} = 0, f_{zz} = 2, f_{xy} = -1, f_{xz} = 0, f_{yz} = 1$, we obtain

$$\begin{aligned}&\sum_{j=1}^{J-1}(f_x e_{F,j-1}^{n+\frac{1}{2}} + f_y e_{F,j}^{n+\frac{1}{2}} + f_z e_{F,j+1}^{n+\frac{1}{2}})e_{F,j}^{n+\frac{1}{2}}\\&= -(f_x e_{F,\bar{x}}^{n+\frac{1}{2}}, e_F^{n+\frac{1}{2}}) + \frac{3}{h}(f_y e_F^{n+\frac{1}{2}}, e_F^{n+\frac{1}{2}}) + (f_z e_{F,x}^{n+\frac{1}{2}}, e_F^{n+\frac{1}{2}}),\end{aligned} \tag{32}$$

$$\begin{aligned}&\sum_{j=1}^{J-1} Q e_{F,j}^{n+\frac{1}{2}} = \frac{1}{2}\sum_{j=1}^{J-1}[f_{xx}(e_{C,j-1}^{n+\frac{1}{2}})^2 + f_{yy}(e_{C,j}^{n+\frac{1}{2}})^2 + f_{zz}(e_{C,j+1}^{n+\frac{1}{2}})^2]e_{F,j}^{n+\frac{1}{2}}\\&+\sum_{j=1}^{J-1}[f_{xy}e_{C,j-1}^{n+\frac{1}{2}}e_{C,j}^{n+\frac{1}{2}} + f_{xz}e_{C,j-1}^{n+\frac{1}{2}}e_{C,j+1}^{n+\frac{1}{2}} + f_{yz}e_{C,j}^{n+\frac{1}{2}}e_{C,j+1}^{n+\frac{1}{2}}]e_{F,j}^{n+\frac{1}{2}}\\&= ((e_C^{n+\frac{1}{2}})_x^2, e_F^{n+\frac{1}{2}}) - ((e_C^{n+\frac{1}{2}})^2, e_{F,x}^{n+\frac{1}{2}}) + (e_{C,x}^{n+\frac{1}{2}}, e_C^{n+\frac{1}{2}}e_F^{n+\frac{1}{2}}) - (e_C^{n+\frac{1}{2}}, (e_C^{n+\frac{1}{2}}e_F^{n+\frac{1}{2}})_x).\end{aligned} \tag{33}$$

Using Lemma 1 and Cauchy–Schwarz inequality, we have

$$\begin{aligned}&\frac{\tau_F}{3}(f_x e_{F,\bar{x}}^{n+\frac{1}{2}}, e_F^{n+\frac{1}{2}}) - \frac{\tau_F}{h}(f_y e_F^{n+\frac{1}{2}}, e_F^{n+\frac{1}{2}}) - \frac{\tau_F}{3}(f_z e_{F,x}^{n+\frac{1}{2}}, e_F^{n+\frac{1}{2}})\\&\le M\tau_F(\|e_{F,x}^{n+\frac{1}{2}}\|^2 + \|e_F^{n+\frac{1}{2}}\|^2),\end{aligned} \tag{34}$$

$$\begin{aligned}&-\frac{\tau_F}{3}((e_C^{n+\frac{1}{2}})_x^2, e_F^{n+\frac{1}{2}}) + \frac{\tau_F}{3}((e_C^{n+\frac{1}{2}})^2, e_{F,x}^{n+\frac{1}{2}})\\&-\frac{\tau_F}{3}(e_{C,x}^{n+\frac{1}{2}}, e_C^{n+\frac{1}{2}}e_F^{n+\frac{1}{2}}) + \frac{\tau_F}{3}(e_C^{n+\frac{1}{2}}, (e_C^{n+\frac{1}{2}}e_F^{n+\frac{1}{2}})_x)\\&\le M\tau_F(\|e_C^{n+\frac{1}{2}}\|_\infty^2\|e_C^{n+\frac{1}{2}}\|^2 + \|e_C^{n+\frac{1}{2}}\|_\infty^2\|e_{C,x}^{n+\frac{1}{2}}\|^2 + \|e_F^{n+\frac{1}{2}}\|^2 + \|e_{F,x}^{n+\frac{1}{2}}\|^2),\end{aligned} \tag{35}$$

$$2\tau_F(Er_F^n, e_F^{n+\frac{1}{2}}) \le \tau_F\|Er_F^n\|^2 + M\tau_F\|e_F^{n+\frac{1}{2}}\|^2. \tag{36}$$

Substituting equations (34)-(35) into (31), then

$$\begin{aligned}&\|e_F^{n+1}\|^2 + \|e_{F,x}^{n+1}\|^2\\&\le \|e_F^n\|^2 + \|e_{F,x}^n\|^2 + M\tau_F(\|\eta_F^{n+1}\|^2 + \|e_F^{n+1}\|^2 + \|e_F^n\|^2 + \|e_{F,x}^{n+1}\|^2 + \|e_{F,x}^n\|^2)\\&\quad + M\tau_F(\|e_C^{n+\frac{1}{2}}\|_\infty^2\|e_C^{n+\frac{1}{2}}\|^2 + \|e_C^{n+\frac{1}{2}}\|_\infty^2\|e_{C,x}^{n+\frac{1}{2}}\|^2) + \tau_F\|Er_F^n\|^2.\end{aligned} \tag{37}$$

Taking the inner product $(\cdot,\cdot)$ on both sides of equation (30) with $\eta_F^{n+1} + \eta_F^n$, we obtain

$$\|\eta_F^{n+1}\|^2 \le \|\eta_F^n\|^2 + M\tau_F(\|e_{F,x}^n\|^2 + \|\eta_F^{n+1}\|^2 + \|\eta_F^n\|^2) + \tau_F\|Es_F^n\|^2. \tag{38}$$

Add equations (37) and (38), we have

$$\begin{aligned}&\|e_F^{n+1}\|^2 + \|e_{F,x}^{n+1}\|^2 + \|\eta_F^{n+1}\|^2 \le \|e_F^n\|^2 + \|e_{F,x}^n\|^2 + \|\eta_F^n\|^2\\&+ M\tau_F(\|\eta_F^{n+1}\|^2 + \|\eta_F^n\|^2 + \|e_F^{n+1}\|^2 + \|e_F^n\|^2 + \|e_{F,x}^{n+1}\|^2 + \|e_{F,x}^n\|^2)\\&+ M\tau_F(\|e_C^{n+\frac{1}{2}}\|_\infty^2\|e_C^{n+\frac{1}{2}}\|^2 + \|e_C^{n+\frac{1}{2}}\|_\infty^2\|e_{C,x}^{n+\frac{1}{2}}\|^2)\\&+ \tau_F\|Er_F^n\|^2 + \tau_F\|Es_F^n\|^2.\end{aligned} \tag{39}$$

Let $B_F^n = \|e_F^n\|^2 + \|e_{F,x}^n\|^2 + \|\eta_F^n\|^2$, then

$$\begin{aligned}B_F^{n+1} - B_F^n \le M\tau_F(B_F^{n+1} + B_F^n) + M\tau_F(\|e_C^{n+\frac{1}{2}}\|_\infty^2\|e_C^{n+\frac{1}{2}}\|^2 + \|e_C^{n+\frac{1}{2}}\|_\infty^2\|e_{C,x}^{n+\frac{1}{2}}\|^2)\\+\tau_F\|Er_F^n\|^2 + \tau_F\|Es_F^n\|^2,\end{aligned}$$

Preprints (www.preprints.org) | NOT PEER-REVIEWED | Posted: 29 May 2023 doi:10.20944/preprints202305.1973.v1

and obtain

$$(1 - M\tau_F)(B_F^{n+1} - B_F^n) \leq 2M\tau_F B_F^n + M\tau_F(h^4 + \tau_C^4 + \tau_F^2).$$

By taking τ_F small enough so that $(1 - M\tau_F) > \lambda > 0$, then

$$B_F^{n+1} - B_F^n \leq M\tau_F(h^4 + \tau_C^4 + \tau_F^2) + M\tau_F B_F^n. \tag{40}$$

Summing from 0 to $N-1$ inequalities in equation (40), we obtain

$$B_F^N \leq B_F^0 + M\tau_F(h^4 + \tau_C^4 + \tau_F^2) + M\tau_F \sum_{n=0}^{N-1} B_F^n. \tag{41}$$

Using Lemma 2, we get

$$B_F^N \leq [B_F^0 + M\tau_F(h^4 + \tau_C^4 + \tau_F^2)]e^{MN\tau_F}. \tag{42}$$

From equation (42) and the initial and boundary condition, we have

$$\|e_F^n\| \leq O(h^2 + \tau_C^2 + \tau_F), \|e_{F,x}^n\| \leq O(h^2 + \tau_C^2 + \tau_F), \|\eta_F^n\| < O(h^2 + \tau_C^2 + \tau_F). \tag{43}$$

Using Lemma 3, it lead to

$$\|e_F^n\|_\infty \leq O(h^2 + \tau_C^2 + \tau_F). \tag{44}$$

This completes the proof of Theorem 2. □

5. Numerical Results

This section provides some numerical examples aimed at demonstrating the accuracy and computational time of the TT-M finite difference scheme that was discussed in Section 3. We consider the SRLW equation as the following form:

$$\begin{aligned}
&u_t + \rho_x + uu_x - u_{xxt} = 0, && -40 \leq x \leq 40,\ 0 < t \leq 4,\\
&\rho_t + u_x = 0, && -40 \leq x \leq 40,\ 0 < t \leq 4,\\
&u(x_L, t) = u(x_R, t) = 0,\ \rho(x_L, t) = \rho(x_R, t) = 0, && 0 < t \leq 4,\\
&u(x, 0) = u_0(x),\ \rho(x, 0) = \rho_0(x), && -40 \leq x \leq 40.
\end{aligned}$$

The exact solitary wave solution [4] of the SRLW equation (1) has the following form

$$u(x,t) = \frac{3(v^2-1)}{v}\operatorname{sech}^2\left(\sqrt{\frac{v^2-1}{4v^2}}(x - vt)\right)$$
$$\rho(x,t) = \frac{3(v^2-1)}{v^2}\operatorname{sech}^2\left(\sqrt{\frac{v^2-1}{4v^2}}(x - vt)\right).$$

In this section, we chose $v = 1.5$ associated with this equation, which takes the form

$$u(x,t) = \frac{5}{2}\operatorname{sech}^2\frac{\sqrt{5}}{6}\left(x - \frac{3}{2}t\right), \quad \rho(x,t) = \frac{5}{3}\operatorname{sech}^2\frac{\sqrt{5}}{6}\left(x - \frac{3}{2}t\right),$$

and consider the following initial conditions

$$u_0(x) = \frac{5}{2}\operatorname{sech}^2\frac{\sqrt{5}}{6}x, \quad \rho_0(x) = \frac{5}{3}\operatorname{sech}^2\frac{\sqrt{5}}{6}x.$$

Preprints (www.preprints.org) | NOT PEER-REVIEWED | Posted: 29 May 2023 doi:10.20944/preprints202305.1973.v1

5.1. Error and convergence rate

We define the error and convergence rate by the following formula:

$$e_m(h,\tau) = \|v^n - u_m^n\|_\infty, \ \ \eta_m(h,\tau) = \|\varphi^n - \rho_m^n\|,$$
$$uRate_m^x = \log_2\left(\frac{e_m(2h,4\tau)}{e_m(h,\tau)}\right), \ \rho Rate_m^x = \log_2\left(\frac{\eta_m(2h,4\tau)}{\eta_m(h,\tau)}\right),$$
$$uRate_m^t = \log_2\left(\frac{e_m(2h,2\tau)}{e_m(h,\tau)}\right), \ \rho Rate_m^t = \log_2\left(\frac{\eta_m(2h,2\tau)}{\eta_m(h,\tau)}\right),$$

where m represents the TT-M finite difference scheme or the standard nonlinear finite difference (SNFD) scheme. We set $\tau_C = 4\tau_F$ in the entire numerical illustration process.

Tables 1 and 2 present discrete norm errors, convergence rates, and the time cost for both the TT-M finite difference scheme and the SNFD scheme. To demonstrate the accuracy of the proposed method, we computed the error of TT-M finite difference scheme at the final time $t = 4$ for various mesh steps and compare it to the errors obtained by the SNFD scheme. The results from the new scheme show nearly identical significant digits as those obtained by the SNFD scheme. In term of the convergence rate, the results indicate that both the SNFD scheme and the TT-M finite difference scheme achieve approximately second-order convergence in space when $\tau_F = h^2$ and first-order in time when $h = \tau_F$, which confirming the theoretical results.

Figures 1 illustrates the exact and numerical solutions of $u(x,t)$ and $\rho(x,t)$ at $t = 4$ obtained by the TT-M finite difference scheme. The results indicate the excellent correspondence between our numerical solution and the exact solution. Furthermore, the CPU times of the two schemes are plotted in Figure 2 under $\tau_F = h^2$ and $h = \tau_F$, respectively. It is worth noting that the TT-M finite difference scheme can significantly decrease computation time. To sum up, the computational performance of the new scheme is obviously better than that of the SNFD scheme.

Table 1. The errors and convergence rates with $\tau_F = h^2$.

SNFD scheme					
(h,τ_F)	$e_{SNFD}(h,\tau_F)$	$uRate^x_{SNFD}$	$\eta_{SNFD}(h,\tau_F)$	$\rho Rate^x_{SNFD}$	**CPU(s)**
$\left(\frac{1}{2},\frac{1}{4}\right)$	8.2798×10^{-2}	—	2.9797×10^{-1}	—	0.14
$\left(\frac{1}{4},\frac{1}{16}\right)$	2.0361×10^{-2}	2.02	7.3503×10^{-2}	2.02	0.51
$\left(\frac{1}{8},\frac{1}{64}\right)$	5.0629×10^{-3}	2.01	1.8306×10^{-2}	2.01	12.30
$\left(\frac{1}{16},\frac{1}{256}\right)$	1.2641×10^{-3}	2.00	4.5719×10^{-3}	2.00	136.31
$\left(\frac{1}{32},\frac{1}{1024}\right)$	3.1597×10^{-4}	2.00	1.1427×10^{-3}	2.00	1943.47
TT-M finite difference scheme					
(h,τ_F)	$e_{TT-M}(h,\tau_F)$	$uRate^x_{TT-M}$	$\eta_{TT-M}(h,\tau_F)$	$\rho Rate^x_{TT-M}$	**CPU(s)**
$\left(\frac{1}{2},\frac{1}{4}\right)$	8.3934×10^{-2}	—	3.0015×10^{-1}	—	0.10
$\left(\frac{1}{4},\frac{1}{16}\right)$	2.0360×10^{-2}	2.04	7.3555×10^{-2}	2.03	0.30
$\left(\frac{1}{8},\frac{1}{64}\right)$	5.0616×10^{-3}	2.01	1.8308×10^{-2}	2.01	7.53
$\left(\frac{1}{16},\frac{1}{256}\right)$	1.2639×10^{-3}	2.00	4.5721×10^{-3}	2.00	76.99
$\left(\frac{1}{32},\frac{1}{1024}\right)$	3.1596×10^{-4}	2.00	1.1427×10^{-3}	2.00	1297.88

Preprints (www.preprints.org) | NOT PEER-REVIEWED | Posted: 29 May 2023 doi:10.20944/preprints202305.1973.v1

Table 2. The errors and convergence rates with $h = \tau_F$.

SNFD scheme					
(h, τ_F)	$e_{SNFD}(h, \tau_F)$	$uRate^t_{SNFD}$	$\eta_{SNFD}(h, \tau_F)$	$\rho Rate^t_{SNFD}$	**CPU(s)**
$\left(\frac{1}{8}, \frac{1}{8}\right)$	3.1920×10^{-2}	—	1.1381×10^{-1}	—	2.47
$\left(\frac{1}{16}, \frac{1}{16}\right)$	1.5552×10^{-2}	1.04	5.5256×10^{-2}	1.04	14.09
$\left(\frac{1}{32}, \frac{1}{32}\right)$	7.6748×10^{-3}	1.02	2.7221×10^{-2}	1.02	109.20
$\left(\frac{1}{64}, \frac{1}{64}\right)$	3.8121×10^{-3}	1.01	1.3509×10^{-2}	1.01	770.01
$\left(\frac{1}{128}, \frac{1}{128}\right)$	1.8997×10^{-3}	1.00	6.7298×10^{-3}	1.00	5792.53
TT-M finite difference scheme					
(h, τ_F)	$e_{TT-M}(h, \tau_F)$	$uRate^t_{TT-M}$	$\eta_{TT-M}(h, \tau_F)$	$\rho Rate^t_{TT-M}$	**CPU(s)**
$\left(\frac{1}{8}, \frac{1}{8}\right)$	3.1962×10^{-2}	—	1.1414×10^{-1}	—	1.49
$\left(\frac{1}{16}, \frac{1}{16}\right)$	1.5540×10^{-2}	1.04	5.5323×10^{-2}	1.04	7.10
$\left(\frac{1}{32}, \frac{1}{32}\right)$	7.6694×10^{-3}	1.02	2.7237×10^{-2}	1.02	51.40
$\left(\frac{1}{64}, \frac{1}{64}\right)$	3.8102×10^{-3}	1.01	1.3513×10^{-2}	1.01	414.33
$\left(\frac{1}{128}, \frac{1}{128}\right)$	1.8991×10^{-3}	1.00	6.7308×10^{-3}	1.01	3289.71

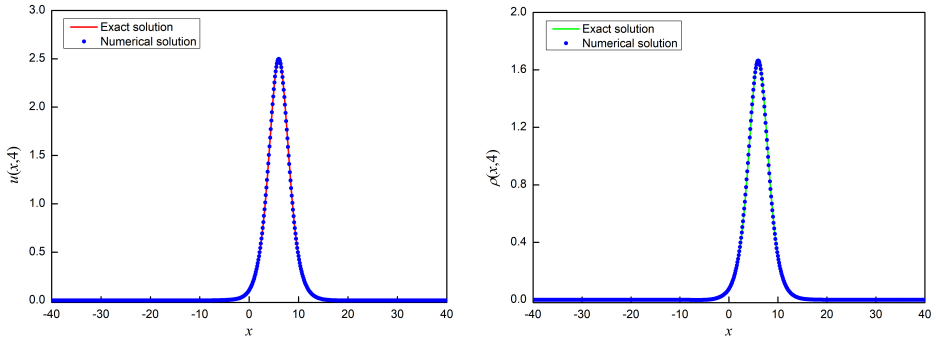

(**a**) (**b**)

Figure 1. Exact and numerical solution of $u(x,t)$ (**a**) and $\rho(x,t)$ (**b**) at $t = 4$.

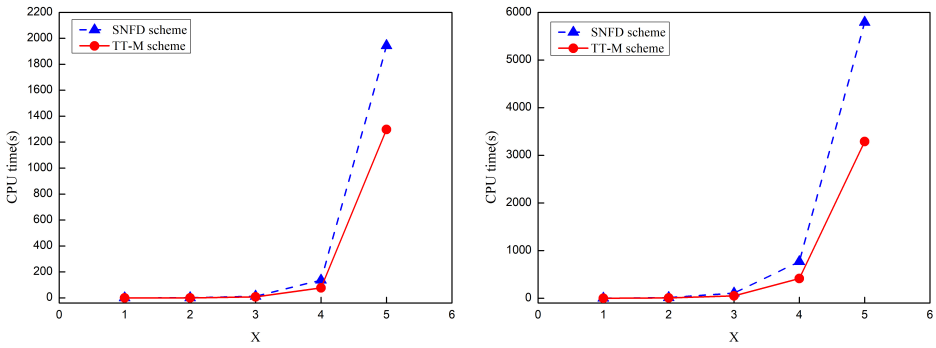

(**a**) (**b**)

Figure 2. Comparison of CPU times with $\tau_F = h^2$ (**a**) and $h = \tau_F$ (**b**) based on the data in Table 1-2.

Preprints (www.preprints.org) | NOT PEER-REVIEWED | Posted: 29 May 2023 doi:10.20944/preprints202305.1973.v1

5.2. Conservative approximations

To further verify the accuracy of the new scheme, we calculate four conservation laws of the SRLW equation (1), such as:

$$Q_1 = \frac{1}{2}\int_{-\infty}^{\infty} \rho dx, \qquad Q_2 = \frac{1}{2}\int_{-\infty}^{\infty} u dx,$$
$$Q_3 = \frac{1}{2}\int_{-\infty}^{\infty} (u^2 + u_x^2 + \rho^2) dx, \quad Q_4 = \frac{1}{2}\int_{-\infty}^{\infty} (\rho u + \frac{1}{6}u^3) dx.$$

Afterwards, employing discrete forms, we are able to compute four approximate conservative quantities which can be represented as

$$Q_1 = \frac{h}{2}\sum_{j=0}^{J-1} \rho_j^n,$$
$$Q_2 = \frac{h}{2}\sum_{j=0}^{J-1} u_j^n,$$
$$Q_3 = \frac{h}{2}\sum_{j=0}^{J-1} (u_j^n)^2 + \frac{1}{2h}\sum_{j=0}^{J-1} (u_{j+1}^n - u_j^n)^2 + \frac{h}{2}\sum_{j=0}^{J-1} (\rho_j^n)^2,$$
$$Q_4 = \frac{h}{2}\sum_{j=0}^{J-1} \rho_j^n u_j^n + \frac{h}{12}\sum_{j=0}^{J-1} (u_j^n)^3.$$

The quantities values are recorded in Tables 3-6. In Tables 3 and 4, regardless of the time step and grid spacing, the quantities Q_1 and Q_2 remain well-preserved at various times. In Table 5, for the case $h = 1/2$ and $\tau_F = 1/4$, one can see that the quantity Q_3 experiences a slight increase as time increases, however, as the spatial and temporal step sizes decrease, the variation of Q_3 becomes extremely small. In Table 6, it has been found that for quantity Q_4, there was a minor decline under different mesh steps, but it gradually rebounded over time. Meanwhile, as the spatial and temporal step sizes decrease, the Q_4 increases slightly. Figure 3 plots the variation curves of four quantities for the case $h = 1/8$ and $\tau_F = 1/64$, which visually demonstrate that our scheme preserves the four conservation laws.

Table 3. Quantities Q_1 under different mesh steps h and τ_F at various times.

TT-M finite difference scheme				
	$(\frac{1}{2}, \frac{1}{4})$	$(\frac{1}{4}, \frac{1}{16})$	$(\frac{1}{8}, \frac{1}{64})$	$(\frac{1}{16}, \frac{1}{256})$
$t = 0.0$	4.4721359549	4.4721359549	4.4721359549	4.4721359549
$t = 0.5$	4.4721359549	4.4721359549	4.4721359549	4.4721359549
$t = 1.0$	4.4721359549	4.4721359549	4.4721359549	4.4721359549
$t = 1.5$	4.4721359549	4.4721359549	4.4721359549	4.4721359549
$t = 2.0$	4.4721359549	4.4721359549	4.4721359549	4.4721359549
$t = 2.5$	4.4721359549	4.4721359549	4.4721359549	4.4721359549
$t = 3.0$	4.4721359549	4.4721359549	4.4721359549	4.4721359549
$t = 3.5$	4.4721359549	4.4721359549	4.4721359549	4.4721359549
$t = 4.0$	4.4721359549	4.4721359549	4.4721359549	4.4721359549

Preprints (www.preprints.org) | NOT PEER-REVIEWED | Posted: 29 May 2023 doi:10.20944/preprints202305.1973.v1

Table 4. Quantities Q_2 under different mesh steps h and τ_F at various times.

TT-M finite difference scheme				
	$(\frac{1}{2}, \frac{1}{4})$	$(\frac{1}{4}, \frac{1}{16})$	$(\frac{1}{8}, \frac{1}{64})$	$(\frac{1}{16}, \frac{1}{256})$
$t = 0.0$	6.7082039324	6.7082039324	6.7082039324	6.7082039324
$t = 0.5$	6.7082039324	6.7082039324	6.7082039324	6.7082039324
$t = 1.0$	6.7082039324	6.7082039324	6.7082039324	6.7082039324
$t = 1.5$	6.7082039324	6.7082039324	6.7082039324	6.7082039324
$t = 2.0$	6.7082039324	6.7082039324	6.7082039324	6.7082039324
$t = 2.5$	6.7082039324	6.7082039324	6.7082039324	6.7082039324
$t = 3.0$	6.7082039324	6.7082039324	6.7082039324	6.7082039324
$t = 3.5$	6.7082039324	6.7082039324	6.7082039324	6.7082039324
$t = 4.0$	6.7082039323	6.7082039323	6.7082039323	6.7082039323

Table 5. Quantities Q_3 under different mesh steps h and τ_F at various times.

TT-M finite difference scheme				
	$(\frac{1}{2}, \frac{1}{4})$	$(\frac{1}{4}, \frac{1}{16})$	$(\frac{1}{8}, \frac{1}{64})$	$(\frac{1}{16}, \frac{1}{256})$
$t = 0.0$	17.3814360100	17.3890764778	17.3909982095	17.3914793723
$t = 0.5$	17.3879364459	17.3894925427	17.3910247524	17.3914810404
$t = 1.0$	17.4021575260	17.3904434452	17.3910850544	17.3914848239
$t = 1.5$	17.4178948195	17.3914089843	17.3911453660	17.3914885933
$t = 2.0$	17.4279575149	17.3919924045	17.3911803618	17.3914907570
$t = 2.5$	17.4320624736	17.3921089940	17.3911854445	17.3914910387
$t = 3.0$	17.4298852213	17.3919072419	17.3911710024	17.3914901056
$t = 3.5$	17.4257242289	17.3915916231	17.3911504036	17.3914888028
$t = 4.0$	17.4208004460	17.3913048704	17.3911324701	17.3914876800

Table 6. Quantities Q_4 under different mesh steps h and τ_F at various times.

TT-M finite difference scheme				
	$(\frac{1}{2}, \frac{1}{4})$	$(\frac{1}{4}, \frac{1}{16})$	$(\frac{1}{8}, \frac{1}{64})$	$(\frac{1}{16}, \frac{1}{256})$
$t = 0.0$	29.8645685095	29.8270800111	29.8174683777	29.8150480627
$t = 0.5$	29.5194998279	29.7377964805	29.7949677954	29.8094115019
$t = 1.0$	29.2953094352	29.6804305056	29.7805099425	29.8057894879
$t = 1.5$	29.2373157339	29.6665651150	29.7770997278	29.8049405034
$t = 2.0$	29.3052034101	29.6864373371	29.7822468973	29.8062391542
$t = 2.5$	29.4333002603	29.7204018949	29.7909264484	29.8084218678
$t = 3.0$	29.5520897511	29.7519209103	29.7989376025	29.8104338587
$t = 3.5$	29.6355327196	29.7733189521	29.8043614200	29.8117950932
$t = 4.0$	29.6765644108	29.7843463859	29.8071613054	29.8124980105

Preprints (www.preprints.org) | NOT PEER-REVIEWED | Posted: 29 May 2023 doi:10.20944/preprints202305.1973.v1

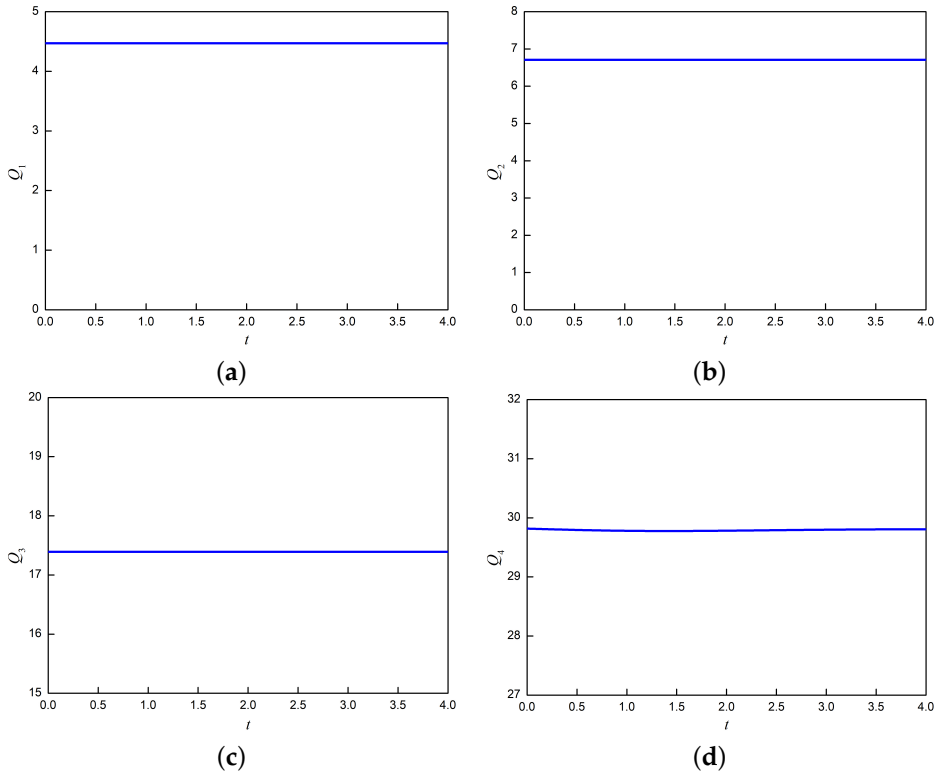

Figure 3. Quantities Q_1 (**a**), Q_2 (**b**), Q_3 (**c**) and Q_4 (**d**) under mesh steps $h = 1/8$, $\tau_F = 1/64$.

6. Conclusions

The paper presents a new time two-mesh finite difference scheme for the nonlinear symmetric regularized long wave equation with a nonlinear term including derivatives. The time interval is divied into coarse and fine meshes, then the Lagrange's linear interpolation formula and Taylor's formula are utilized to construct the three steps time two-mesh finite difference scheme. The convergence of the new scheme are also analyzed and theoretical results are verified by some numerical examples. Compared to the standard nonlinear finite difference scheme, our scheme not only maintains accuracy but also reduces CPU time. Therefore, the TT-M finite difference scheme is a promising method for solving the SRLW equation.

Author Contributions: Conceptualization, J.G.; methodology, J.G.; software, J.G. and S.H.; validation, S.H., Q.B. and J.L.; formal analysis, J.G. and S.H.; writing—original draft preparation, J.G.; writing—review and editing, J.G., S.H.; funding acquisition, S.H., Q.B and J.L. All authors have read and agreed to the published version of the manuscript.

Funding: This work is supported by National Natural Science Foundation of China (Nos. 12161034 and 11961022), Natural Science Foundation of Inner Mongolia (No. 2021MS01017), Natural Scientific Research Innovation Team of Hohhot Minzu College (No. HMTD202005).

Institutional Review Board Statement: Not applicable.

Informed Consent Statement: Not applicable.

Data Availability Statement: All the data were computed using our method.

Acknowledgments: We are grateful to the anonymous reviewers for their valuable suggestions and comments.

Conflicts of Interest: The authors declare that the research was conducted in the absence of any commercial or financial relationships that could be construed as a potential conflict of interest.

References

1. Peregrine, D. H. Calculations of the development of an undular bore. *Journal of Fluid Mechanics* **1966**, *25*, 321–330.
2. Peregrine, D. H. Long waves on beach. *Journal of Fluid Mechanics* **1967**, *27*, 815-827.
3. Korteweg, D.J.; de Vries, G. On the change of form of long waves advancing in a rectangular canal, and on a new type of long stationary waves. *Philosophical Magazine* **1895**, *39*, 422-443.
4. Seyler, C.E.; Fenstermacher, D.L. A symmetric regularized-long-wave equation. *Physics of Fluids* **1984**, *27*, 4–7.
5. Wang, T.C.; Zhang, L.M.; Chen, F.Q. Conservative schemes for the symmetric regularized long wave equations. *Applied Mathematics and Computation* **2007**, *190*, 1063-1080.
6. Yimnet, S.; Wongsaijai, B.; Rojsiraphisal, T.; Poochinapan, K. Numerical implementation for solving the symmetric regularized long wave equation. *Applied Mathematics and Computation* **2016**, *273*, 809-825.
7. Hu, J.S.; Zheng, K.L.; Zheng, M.B. Numerical simulation and convergence analysis of high-order conservative difference scheme for SRLW equation. *Applied Mathematical Modelling* **2014**, *38*, 5573-5581.
8. Li, S.G. Numerical study of a conservative weighted compact difference scheme for the symmetric regularized long wave equations. *Numerical Methods for Partial Differential Equations* **2019**, *35*, 60-83.
9. Bai, Y.; Zhang L.M. A conservative finite difference scheme for symmetric regularized long wave equations. *Acta Mathematicae Applicatae Sinica* **2007**, *30*, 248–255.
10. Xu, Y.C.; Hu, B.; Xie, X.P.; Hu J.S. Mixed finite element analysis for dissipative SRLW equations with damping term. *Physics of Fluids* **2012**, *218*, 4788-4797.
11. He, Y.Y.; Wang, X.F.; Cheng, H.; Deng, Y.Q. Numerical analysis of a high-order accurate compact finite difference scheme for the SRLW equation. *Applied Mathematics and Computation* **2022**, *418*, 126837.
12. Liu, Y.; Yu, Z.D.; Li, H.; Liu, F.W.; Wang, J.F. Time two-mesh algorithm combined with finite element method for time fractional water wave model. *International Journal of Heat and Mass Transfer* **2018**, *120*, 1132–1145.
13. Yin, B.L.; Liu, Y.; Li, H.; He, S. Fast algorithm based on TT-M FE system for space fractional Allen-Cahn equations with smooth and non-smooth solutions. *Journal Of Computational Physics* **2019**, *379*, 351–372.
14. Liu, Y.; Fan, E.Y.; Yin, B.L.; Li, H.; Wang, J.F. TT-M finite element algorithm for a two-dimensional space fractional Gray-Scott model. *Computers and Mathematics with Applications* **2020**, *80*, 1793–1809.
15. Wen, C.; Liu, Y.; Yin, B.L.; Li, H.; Wang, J.F. Fast second-order time two-mesh mixed finite element method for a nonlinear distributed-order sub-diffusion model. *Numerical Algorithms* **2021**, *88*, 523–553.
16. Tian, J.L.; Sun, Z.Y.; Liu, Y.; Li, H. TT-M Finite Element Algorithm for the Coupled Schrödinger–Boussinesq Equations. *Axioms* **2022**, *11*, 314.
17. Qiu, W.L.; Xu, D.; Guo, J.; Zhou, J. A time two-grid algorithm based on finite difference method for the two-dimensional nonlinear time-fractional mobile/immobile transport model. *Numerical Algorithms* **2020**, *85*, 39–58.
18. Xu, D.; Guo, J.; Qiu, W.L. Time two-grid algorithm based on finite difference method for two-dimensional nonlinear fractional evolution equations. *Applied Numerical Mathematics* **2019**, *152*, 169–184.
19. Niu, Y.X.; Liu, Y.; Li, H.; Liu, F.W. Fast high-order compact difference scheme for the nonlinear distributed-order fractional Sobolev model appearing in porous media. *Mathematics and Computers in Simulation* **2023**, *203*, 387-407.
20. He, S.; Liu, Y.; Li, H.. Numerical simulation and convergence analysis of high-order conservative difference scheme for SRLW equation. *Entropy* **2022**, *24*, 806.
21. Zhou, Y.L. *Application of Discrete Functional Analysis to the Finite Difference Method*; International Academic Publishers: Beijing, China, 1990.